EUROGRAPHICS 2008 / G. Drettakis and R. Scopigno
(Guest Editors)

Volume 27 (2008), Number 2

Characterization for High Dynamic Range Imaging

Min H. Kim† and Jan Kautz‡

Department of Computer Science, University College London


Before HDR characterization


After HDR characterization


Difference map (mid-gray = mean) amplified by 10

Abstract

In this paper we present a new practical camera characterization technique to improve color accuracy in high dynamic range (HDR) imaging. Camera characterization refers to the process of mapping device-dependent signals, such as digital camera RAW images, into a well-defined color space. This is a well-understood process for low dynamic range (LDR) imaging and is part of most digital cameras — usually mapping from the raw camera signal to the sRGB or Adobe RGB color space. This paper presents an efficient and accurate characterization method for high dynamic range *imaging that extends previous methods originally designed for LDR imaging. We demonstrate that our characterization method is very accurate even in unknown illumination conditions, effectively turning a digital camera into a measurement device that measures physically accurate radiance values — both in terms of luminance and color — rivaling more expensive measurement instruments.*

Categories and Subject Descriptors (according to ACM CCS): I.3.3 [Computer Graphics]: Picture/Image Generation I.4.1 [Image Processing and Computer Vision]: Digitization and Image Capture

1. Introduction

Recent advances in high dynamic range (HDR) imaging allow us to easily obtain radiance maps with off-the-shelf digital cameras by combining multiple exposures into a single HDR image [MP95, DM97, MN99, RBS99]. These acquired radiance maps are commonly used as environment maps for lighting simulations or for computational photography applications. However, the radiometric accuracy of the acquired HDR radiance maps — both in terms of luminance and color — has rarely been discussed or evaluated because traditional characterization methods for low dynamic range (LDR) imaging [MVPC00, PAJ01, MJ02, MVPC03, ISO06, NFG07] were not designed to characterize HDR radiance maps. We propose a new camera characterization method that works well for HDR imaging, is more accurate than many of the LDR methods and is very efficient in terms of acquisition time and cost. Our method is based on the insight that common reflective targets have two main drawbacks: 1) they only offer a low dynamic range, which makes them not a good choice for HDR imaging and 2) characterization based on reflective targets requires both the reflectance of the target and the spectrum of the illuminant to be known. We therefore propose to use a novel back-lit transparent target specifically designed for HDR imaging, offering a higher dynamic range and wider color gamut. Our method only requires the emitted radiance to be known, which can be easily measured once using a spectroradiometer. This enables us to accurately characterize digital cameras used for HDR imaging. We show the effectiveness of the new method by characterizing three different digital cameras. The achieved accuracy of the cameras is similar to the accuracy of a spectroradiometer. As we will demonstrate, radiance maps acquired by different

† e-mail: m.kim@cs.ucl.ac.uk
‡ e-mail: j.kautz@cs.ucl.ac.uk

cameras are virtually the same when using our characterization method.

2. Background and Related Work

In this section we explain the necessary background and briefly discuss previous techniques.

2.1. Characterization of Digital Cameras

The sensing area of digital cameras consists of a charge coupled device (CCD) where incident photons cause charge to accumulate at each pixel on the sensor. This charge is transferred into an output digital signal via an analogue-to-digital converter [Yam06]. The amount of digitized electronic charge is linear to irradiance on the sensing area — excluding the *noise floor* (fixed-pattern noise, sensor dark current, etc. [Hol98, Jan01]) and *blooming* (overflowing) of the sensor response. Typically, a non-linear function is applied to improve the dynamic range of the camera and at the same time this also takes care of gamma-correction for display.

The sensor is usually mosaiced with an RGB color filter set, which simulates the trichromatic responses (color-matching function) of the human visual system (HVS). *Camera characterization is defined as the transform of device-dependent signals into device-independent coordinates* [Joh02] like CIE XYZ tristimulus values. Ideally, the same mapping works for all types of illuminations.

The trichromatic response value, R, G, and B, of a specific pixel on the sensor is given as the integral of the product of the spectral power distribution of the light source $L(\lambda)$, the reflectance (or transmittance) of the imaged object $\rho(\lambda)$, and the spectral responsivities of the color filters $D_{r/g/b}(\lambda)$ — assuming that incident light is reflected from object surfaces:

$$\begin{aligned} R &= \int L(\lambda)\rho(\lambda)D_r(\lambda)d\lambda \\ G &= \int L(\lambda)\rho(\lambda)D_g(\lambda)d\lambda \\ B &= \int L(\lambda)\rho(\lambda)D_b(\lambda)d\lambda \end{aligned} \tag{1}$$

The integration is taken over a suitable wavelength range in the visible part of the spectrum, for instance, from 380nm to 780nm [ISO06]. The calculation of these response values is similar to the computation of device-independent tristimulus values, such CIE XYZ:

$$\begin{aligned} X &= \int L(\lambda)\rho(\lambda)\bar{x}(\lambda)d\lambda \\ Y &= \int L(\lambda)\rho(\lambda)\bar{y}(\lambda)d\lambda \\ Z &= \int L(\lambda)\rho(\lambda)\bar{z}(\lambda)d\lambda \end{aligned} \tag{2}$$

where $\bar{x}(\lambda)$, $\bar{y}(\lambda)$ and $\bar{z}(\lambda)$ are the CIE color matching functions (CMF) [CIE86]. The only difference between Equation 1 and 2 is the use of different weighting functions $D_{r/g/b}$ and $\bar{x}, \bar{y}, \bar{z}$.

Various camera characterization techniques have been proposed to find a mapping between these color spaces. They can be categorized into two main classes: models based on targets with known reflectances [PAJ01,MJ02,Joh02,ISO06] and models based on the measurement of spectral responsivity using a monochromatic light source [MVPC00, MJ02, MVPC03, ISO06, NFG07].

The reflectance-based techniques use a color target, such as the GretagMacbeth ColorChecker, where the tristimulus values of each color patch are measured first or already known (e.g., in CIE XYZ). A picture of the color target is then taken and a direct mapping between the image's RGB-values and the measured XYZ values is derived via linear regression (or polynomial regression in case of non-linearized images). While these techniques are very simple, they are only valid for the current illumination condition [ISO06], as $L(\lambda)$s in Equation 1 and 2 are not the same with these methods ($L(\lambda)$ in Equation 1 is the spectrum of the light source at scene; $L(\lambda)$ in Equation 2 is usually CIE D50 illuminant in colorimetry and ICC profiles). As soon as the lighting changes, a new mapping is required. Therefore this characterization method is very limited. Nonetheless it is universally used for ICC input profiles [ICC04] and is part of the ISO standard [ISO06]. Reflectance-based techniques have also been extended to HDR imaging by assembling characterized LDR images into an HDR image by using the ICC method [GHS01]. However, this extension shares the same assumption of fixed geometric and spectral illumination characteristics, and also does not allow to characterize absolute luminance.

The monochromator-based techniques use a white integrating sphere of known reflectance and a monochromatic light source, whose wavelength can be adjusted. By illuminating the integrating sphere with every single wavelength within the visible spectrum, the spectral responsivity $D_{r/g/b}$ can be measured directly, which then again allows one to derive a simple linear mapping to CIE XYZ. In this case, $L(\lambda)$ is the same for Equation 1 and 2. While this method is much more universal than reflectance-based techniques, monochromator-based techniques are very time-consuming, as each wavelength must be measured individually and a picture needs to be taken for every wavelength. These techniques can in theory be used for camera characterization in HDR imaging. However, only color could be characterized and not luminance, as the employed illumination and target only offers a low dynamic range.

We propose a new technique, which offers the simplicity of reflectance-based techniques with the accuracy and the universal applicability of monochromator-based techniques. Furthermore, it is well-suited for HDR imaging, and can characterize both color and luminance. In fact, our experiments show that a digital camera, characterized with our method, can perform almost identical measurement of the color and luminance information to a spectroradiometer that we tested.

2.2. Acquisition of Radiance Maps

In case of most DSLR cameras, the linear digital signals can actually be output before non-linear processing as a *RAW* image. Within the possible range of camera signals, these RAW images correspond to the amount of charge of all the incident photons on the sensor, effectively measuring scene radiance at each pixel.

Figure 1 demonstrates this; the RAW CCD signals and the HDR image are indeed proportional to measured luminance. Consequently, a relative HDR radiance map can be computed by accumulating exposure-scaled linear responses when using linear RAW images. However, if these are not available, the non-linear response curve, which comes from internal camera post-processing such as gamma correction, must be calibrated in order to convert back to linear signals, for which various methods exist [MP95, DM97, MN99]. In this work, we use linear signals avoiding curve fitting and its potential inaccuracies. The acquired luminance levels that are stored in the radiance map are only proportional to physical luminance. Absolute luminance levels can be acquired by re-scaling the luminance values according to a luminance meter [KGS05, IG04]. In contrast, our method calibrates luminance and color at the same time.

2.3. Tone Reproduction Operators

The dynamic range of HDR radiance maps is usually much higher than that of typical displays and cannot be displayed directly. Since simple linear scaling and gamma correction does not achieve satisfactory results when displaying HDR images, tone-mapping algorithms have been introduced that compress the dynamic range in a more suitable manner among a global, local, or perceptual fashion. Since we only deal with the input side of HDR imaging, tone-mapping as well as color appearance modeling is beyond the scope of this paper. However, we use tone-mapping to display our characterized images [RSSF02].

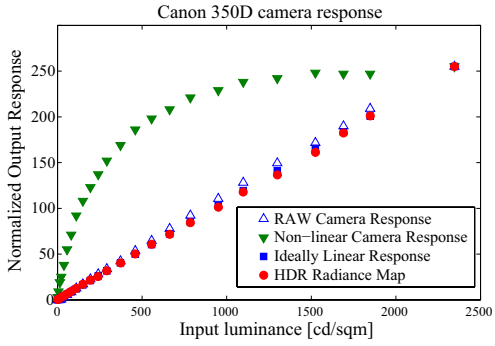

Figure 1: *Characteristic curves of: ordinary non-linear response of Canon 350D, RAW CCD response from the camera, and HDR radiance map on green channel. The Y axis, which signifies the acquired response, is normalized into [0,255]. The X axis represents luminance measured by a spectroradiometer. The square points on the diagonal show the ideally linear response. As the plot shows, the RAW response and the computed HDR radiance map are proportional to incident light.*

3. Camera Characterization for HDR imaging

We will now detail our technique for camera characterization.

3.1. HDR Image Acquisition

Our characterization method can be applied to devices that directly record HDR images or to standard digital cameras that require multi-exposure sequences to be fused into one HDR image. Our HDR imaging setup is based on multi-exposure sequences. We fuse 16-bit RAW camera images, which directly record the linear camera response *without* white-balancing, gamma-correction, or any other processing. HDR images are reconstructed from 18 images taken with varying exposure setting of shutter speed in one f/stop (1/4000-30s) but fixed aperture size (f/11) and film speed (ISO 200), using only the HDR assembly part of Debevec and Malik's method [DM97]. The result of this procedure is a single linear HDR image, which is uncalibrated in terms of absolute luminance and color.

3.2. HDR Characterization

As mentioned earlier, previous characterization methods were either limited to known illumination conditions [PAJ01, MJ02, Joh02, ISO06] or required expensive equipment and prohibitive measurement times [MVPC00, MJ02,MVPC03,ISO06,NFG07]. Furthermore, these characterization methods were really geared towards low dynamic range imaging.

Our technique is based on two insights. First, the product of the spectral power distribution of the light source $L(\lambda)$ and the reflectance of the calibration target $\rho(\lambda)$ can be measured in a single step using a spectroradiometer, allowing camera characterization rather efficient both in terms of cost and measurement time. Second, a novel back-lit transparent target specifically optimized for HDR imaging has larger gamut and higher dynamic range than ordinary reflective targets, making the characterization perform rather accurate measurement of luminance and color and is applicable even in unknown illumination conditions.

3.2.1. Setup

We created our own transparent targets by photographically enlarging the IT8.7/1 [ANS99] color chart onto Kodak Ektachrome professional film (8-by-10 inch) such that each patch matches the sensing area of the employed spectroradiometer (approx. 8mm in diameter). Two enlarged identical targets, under one of which we placed three sheets of neutral density ($2\times$) filters, are placed on a uniform light emitting table in a darkroom to produce a *training set* with plenty of colors (576 patches) and a dynamic range of 4.53 orders of

magnitude. Using a transparent target not only offers a high dynamic range, but also provides a very wide color gamut, see Figure 2.

Two GretagMacbeth ColorChecker targets and two 800W halogen light sources are used to produce a *test set* with 48 color patches, producing a different illumination condition (two halogen lights illuminating one target). The emitted/reflected radiance of each patch in these two experimental sets were measured with the spectroradiometer (Jeti Specbos 1200) of which luminance accuracy is ± 0.05 at $1000 cd/m^2$ and chromaticity repeatability is ± 0.0005 (x,y) [MBG04].

Finally, we took HDR images of these two datasets using three different digital cameras for characterization (Canon 350D, Nikon D100, and Nikon D40), see Figure 3.

3.2.2. Characterization

In traditional colorimetry $L(\lambda)$ refers to *relative* spectral power distributions, which are always normalized (into 100 at 560nm [Hun98]). This discards the intensity scale of the illumination, which is why previous characterization models have difficulties calibrating absolute scales. Furthermore, when tristimulus reflectance values are measured by a spectrophotometer (e.g., the GretagMacbeth Spectrolino), a calibrated tungsten light is used, which is then converted into a CIE D50 illuminant $L_{D50}(\lambda)$ (Eq. 2). However, the scene illuminant $L(\lambda)$ (Eq. 1) is different from that, effectively building in this mismatch into the characterization, which poses problems when different scene illumination is used after characterization. Hence, our technique uses identical $L(\lambda)$ and absolute spectral power distributions to solve both scale and illumination problems.

Using the above setup, we know the emitted radiance values for each patch of our transparent target (measured using the spectroradiometer), corresponding to Equation 2. Furthermore, the linear camera response for each patch is known from the HDR image (corresponding to Equation 1). Since the illumination is identical for both, we can now find a (least-squares) linear transform between the RGB camera response and the physical CIE XYZ radiance values that is applicable to unknown lighting (the $L(\lambda)$ cancels out):

$$X = (A^t A)^{-1} A^t M, \tag{3}$$

where X is a 3×3 transform for characterization, A is a matrix containing the linear RGB camera response for each patch, and M is a matrix containing the measured radiometric CIE XYZ values for each patch.

This transform X can now be used to map any (high dynamic range) RGB value into a physically meaningful CIE XYZ value, independent of the illumination. In our particular setup we find three transforms, one for each digital camera.

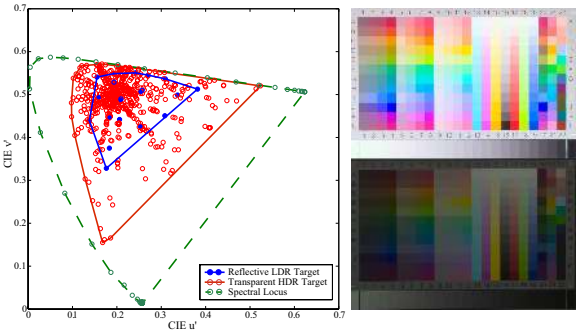

Figure 2: *Comparison of measured gamut boundaries. The transparent HDR target provides a considerably larger color gamut than the ordinary reflective target (GretagMacbeth ColorChecker). Each side of our target (as seen on the right) is an enlarged IT8.7/1 [ANS99] color chart on Kodak Ektachrome professional film (8-by-10 inch).*

3.2.3. Display of Radiance Maps

Our mapping transforms HDR input images into physically meaningful CIE XYZ values. However, in case an image is not intended for measurement purposes but for display, we need to take the human visual system into account, which adapts to a given illumination condition. This is a classical issue and is traditionally called *white balancing*. There are a variety of techniques available to simulate this adaption [HHF99, FB93, FHH97]. For our examples, we use the Bradford chromatic adaptation model used in CIECAM97s; however, any other method can be used as well.

4. Results

We have tested our HDR characterization methods with three different cameras (Nikon D100, Canon 350D, and

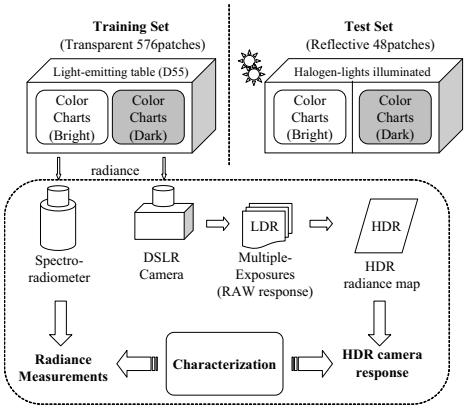

Figure 3: *Setup of characterization. A back-lit transparent color target is captured by a digital camera and all its color patches are measured using a spectroradiometer, which forms the training set that is used to compute the characterization model. A second test set is acquired for validation purposes. It consists of two GretagMacbeth color charts illuminated by halogen light.*

Nikon D40). For this we have computed three characterization models, one for each camera, as described in the previous section (using our transparent color target, see Figure 2).

Table 1 presents the matrices of the linear transform from camera HDR into CIE XYZ coordinates, which were computed as outlined in Section 3.2.2. Note that these matrices not only transform colorimetric information but also luminances, because we take absolute scales into account such that the characterized coordinates are identical to the physical radiance measurement. However, the scale of the matrices may be different for other HDR assembly algorithms.

	Canon 350D / 18-55mm lens			Nikon D40 / 18-55mm lens		
	R	G	B	R	G	B
X	6.8364	1.1685	0.3256	12.9566	1.6246	0.8274
Y	3.0657	4.1205	-1.2861	6.0406	6.4671	-1.5985
Z	0.3650	-0.6863	6.3905	0.5537	-0.9170	11.5996
	Nikon D100 / 35mm lens			Averaged		
	R	G	B	R	G	B
X	10.1001	1.4246	0.5921	9.9644	1.4059	0.5817
Y	4.6565	5.2054	-1.5151	4.5876	5.2643	-1.4666
Z	0.4985	-0.7648	10.1364	0.4724	-0.7894	9.3755

Table 1: *Transformation matrices from camera HDR into CIE XYZ. The transforms were computed from HDR radiance maps of our transparent target and the corresponding radiance measurements.* Averaged *refers to the mean matrix of the three different cameras.*

4.1. Color Accuracy

We analyze the radiometric accuracy of each of the three characterization models (one for each camera) by comparing their results against physical measurements from the spectroradiometer. For each comparison, we compute three different error measures in order to judge the accuracy. First, we compute CIEDE2000 [CIE01]-values, which are commonly used to compare colors in a perceptual fashion. It is based on the CIE LAB color space [CIE86], and as such is really only valid for low dynamic range values. Nonetheless, we include it for completeness. Second, we compute CIE $Yu'v'$ coordinates [CIE86] for the characterized HDR image as well as the measurements from the spectroradiometer, and compute (relative) median differences between them. And third, we compute the (relative) median differences between the characterized CIE XYZ values and the measured CIE XYZ values.

(a)

Training Set	ΔE_{00}	Y	$u'v'$	XYZ
Canon 350D	1.121	0.103	0.013	0.116
Nikon D100	1.311	0.096	0.022	0.117
Nikon D40	1.486	0.066	0.026	0.083

(b)

Test Set	ΔE_{00}	Y	$u'v'$	XYZ
Canon 350D	0.480	0.094	0.016	0.114
Nikon D100	3.816	1.457	0.035	1.660
Nikon D100 (IR filter)	1.615	1.193	0.048	1.439
Nikon D40	3.104	1.159	0.038	1.192

(c)

Test Set – Other Methods	ΔE_{00}	Y	$u'v'$	XYZ
Canon 350D (LDR Char.)	7.028	0.225	0.039	0.228
Canon 350D (HDR ICC)	4.130	1.085	0.073	0.919

Table 2: *Color accuracy of our method: (a) the* Training Set *presents the accuracy of our characterization models using the training data (576 patches under 5571K illumination). (b) the* Test Set *shows the accuracy of the same characterization models using a different test data-set (reflective target under 2946K illumination). Accuracy of other methods (c): LDR characterization (only one target is used [ISO06]) and HDR assembly using ICC profiles [GHS01]. ΔE_{00} denotes the median CIEDE2000 over all patches between measurement and prediction;* Y *shows the median relative differences of luminance levels; $u'v'$ indicates the median relative differences between measurement and prediction of all patches in CIE $u'v'$.* XYZ *shows the median relative differences of CIE XYZ channels between measurement and prediction.* IR filter *means using the infrared blocking filter.*

We first perform these comparisons within the training set (the transparent target, see Figure 2), i.e., we validate that a linear characterization model is sufficient. To this end, we take the original HDR images (one for each camera), convert them to CIE XYZ with the characterization matrices from Table 1 and compute the CIEDE2000 values, $Yu'v'$ median differences, and CIE XYZ median differences for each color patch in the transparent target. As can be seen in Table 2(a), the errors are quite low.

Furthermore, we validate how well the characterization models work with test scenes that were taken under different illumination. Our first test scene consists of two Col-

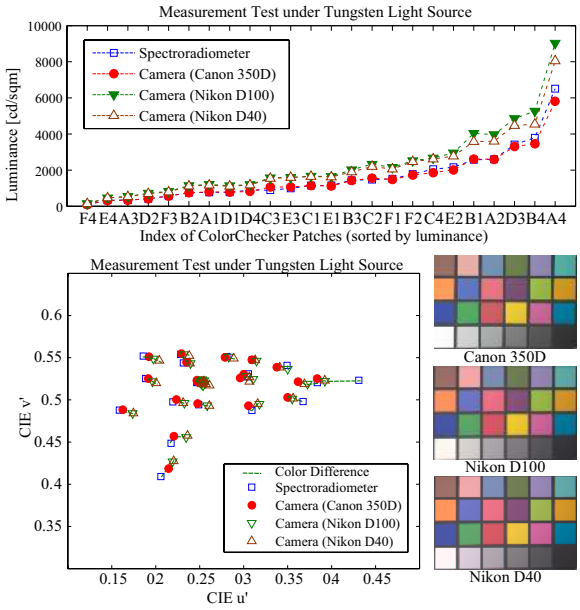

Figure 4: *Test scene consisting of GretagMacbeth charts under halogen light, acquired by three different digital cameras and then characterized using our method. The top plot presents luminance differences between radiometric measurement and camera measurements. In particular the Canon 350D shows very similar performance to the spectroradiometer. Tone-mapped versions of the three characterized images are shown on the right; differences between them are difficult to spot. For a quantitative comparison, see Table 2(b). The bottom left plot shows chromaticity differences of the test patches in a CIE uniform chromaticity diagram. Differences are minor, only one color shows a big difference, which is located outside the camera's R/G/B filter gamut.*

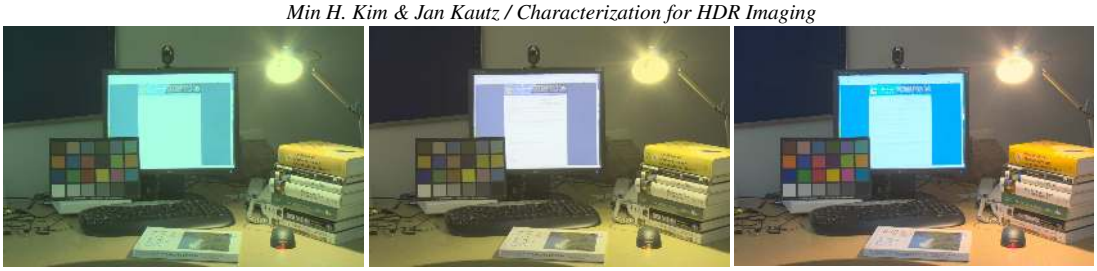

Direct CCD Response (RAW) | Absolute CIE XYZ | Characterization Result

Figure 5: *Each step of our characterization method.* Direct CCD response RAW *is the acquired RAW image without any white balancing. The greenish appearance is due to the infrared filter in front of the CCD, which will be taken care of by the derived mapping.* Absolute CIE XYZ *is the characterized CIE XYZ image (which we render using a 1:1 mapping to RGB for illustration purposes).* Characterization Result *is the final image by mapping from characterized and device-independent CIE XYZ to the display sRGB color space.*

Canon 350D | Nikon D100 | Nikon D40

Figure 6: *An HDR desk scene is characterized with our method for three different digital cameras. Even though they are taken in slightly different perspective and angles, there are only very minor color differences between the images.*

orChecker charts illuminated under halogen light, see Figure 4. As can be seen again in Table 2(b), the errors are quite low, especially for the Canon 350D. We compare this result with the previous reflectance-based LDR characterization [ISO06] technique and the HDR assembly method using ICC profiles [GHS01] (generated by GretagMacbeth ProfileMaker), see Table 2(c) and Figure 7. As predicted, the achieved accuracy is lower than with our new method.

In order to confirm repeatability, we acquired the test set (Canon 350D) a second time under different illumination (2983K). The median ΔE_{00} was 0.546 over 48 patches, which is very close to the ΔE_{00} of 0.480 for the first test set. The Nikon cameras have a slightly higher error, which we could trace back to an inferior infrared filter. Halogen light emits a large amount of infrared light, which caused the HDR images acquired with the Nikon cameras to have a considerable amount of infrared glare. Using an additional infrared blocking filter (Rosco Thermal Shield) in front of the lights yielded a median ΔE_{00} of 1.6 for the Nikon D100, down from 3.8 (see Table 2(b)).

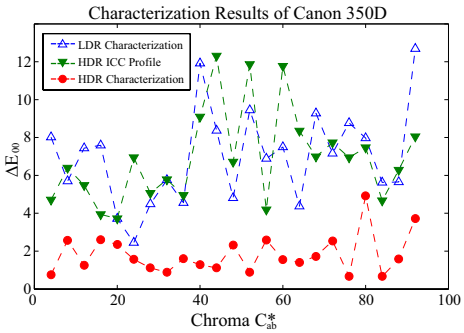

Figure 7: *Comparison of color difference (test set, patches sorted by chromaticity). ΔE_{00} is computed by using a ColorChecker chart in brightly illuminated area. LDR characterization is calculated using the reflectance-based method [ISO06]; the HDR ICC method is according to [GHS01]. Our HDR characterization shows considerably low errors.*

Our second test scene is a desk scene illuminated mainly by a fluorescent desk lamp, see Figure 5 and 6. Tone-mapped versions of the characterized HDR images are shown and as can be seen the colors of all three images are almost identical, even though they were taken with three different cameras.

4.2. Discussion

Our characterization method is applicable to HDR imaging, which is very useful in graphics but also other scientific fields. Our mathematical method of characterization is rather simple—a linear transformation between color spaces—and not different from previous methods. However, our *characterization methodology*, the combination of a new transparent color target, HDR imaging, and characterization theory, solves shortcomings of previous characterization methods.

As shown in the results, our characterization performance is considerably better than previous methods [PAJ01, MJ02,

Joh02, ISO06, GHS01], yet efficient in terms of cost and acquisition time.

However, there are some limitations of our method. The performance depends on the optical quality of the digital camera, including lens flare, vignetting, veiling glare, and the infrared filter. HDR veiling glare can be solved [TAHL07] but acquisition complexity is greatly increased. The measurement used in our method returns radiometric XYZ values, not radiance in each wavelength. In this way, it still allows potential measurement errors with metameric colors like other target-based models.

5. Conclusion

We have presented a new technique that can be utilized to characterize HDR imaging systems, both in terms of luminance and color. It is more accurate than previous reflectance-based characterization methods and less time-consuming than monochromator-based techniques, which were also really only designed for LDR imaging. We have validated the method's accuracy using three different digital cameras and two test data sets. Even though we have devised our method with HDR imaging in mind, the same technique can also be applied to characterize LDR devices.

References

[ANS99] ANSI: *Graphic Technology - Color Transmission Target for Input Scanner Calibration*. Tech. Rep. ANSI IT8.7/1-1993 (R1999), ANSI, 1999.

[CIE86] CIE: *Colorimetry*. Publication CIE 15.2-1986, Commission Internationale de l'Eclairage (CIE), Vienna, 1986.

[CIE01] CIE: *Improvement to Industrial Colour Difference Equation*. Publication CIE 142, CIE, Vienna, 2001.

[DM97] DEBEVEC P. E., MALIK J.: Recovering high dynamic range radiance maps from photographs. In *Proc. ACM SIGGRAPH 97* (Aug 1997), pp. 369–378.

[FB93] FAIRCHILD M. D., BURNS R. S.: Image colour appearance colour specification through extension of cielab. *Colour Research Application* (1993).

[FHH97] FINLAYSON G. D., HUBEL P. M., HORDLEY S.: Colour by correlation. In *Proc. CIC* (1997), IS&T, pp. 6–11.

[GHS01] GÖESELE M., HEIDRICH W., SEIDEL H.-P.: Color calibrated high dynamic range imaging with ICC profiles. In *Proc. CIC* (2001), IS&T, pp. 286–290.

[HHF99] HUBEL P., HOLM J., FINLAYSON G.: Illuminant estimation and colour correction. In *Colour Imaging*, McDonald L., Luo R., (Eds.). John Wiley, Chichester, 1999, pp. 73–95.

[Hol98] HOLST G. C.: *CCD Arrays, Cameras, and Displays*, 2nd ed. JCD Publishing, Bellingham, 1998.

[Hun98] HUNT R. W. G.: *Measuring Colour*, 3rd ed. Fountain Press, Kingston-upon-Thames, 1998.

[ICC04] *International Color Consortium Specification*. Tech. Rep. ICC.1:2004-10, International Color Consortium, 2004.

[IG04] INANICI M., GALVIN J.: *Evaluation of High Dynamic Range Photography as a Luminance Mapping Technique*. Paper LBNL-57545, LBNL, Dec. 2004.

[ISO06] ISO: *ISO/17321-1:2006: Graphic technology and photography — Colour characterisation of digital still cameras (DSCs) — Part 1: Stimuli, metrology and test procedures*. 2006.

[Jan01] JANESICK J. R.: *Scientific Charge-Coupled Devices*, 1st ed. SPIE Publications, Bellingham, 2001.

[Joh02] JOHNSON T.: Methods for characterizing colour scanners and digital cameras. In *Colour Engineering*, Green P., MacDonald L., (Eds.). John Wiley, Chichester, 2002, pp. 165–178.

[KGS05] KRAWCZYK G., GOESELE M., SEIDEL H.-P.: *Photometric Calibration of High Dynamic Range Cameras*. Research Rep. MPI-I-2005-4-005, MPI Informatik, Saarbrücken, Apr. 2005.

[MBG04] MORGENSTERN T., BORNHOEFT G., GOERLICH S.: *Miniaturized Spectroradiometer*. Light 2004, JETI Technische Instrumente GmbH, Brno, Jun. 2004.

[MJ02] MACDONALD L., JI W.: Colour characterisation of a high-resolution digital camera. In *Proc. IS&T CGIV* (2002), vol. 1, pp. 433–437.

[MN99] MITSUNAGA T., NAYAR S. K.: Radiometric self calibration. In *Proc. IEEE CVPR* (Jun. 1999), pp. 374–380.

[MP95] MANN S., PICARD R. W.: *On being 'undigital' with digital cameras: Extending Dynamic Range by Combining Differently Exposed Pictures*. Tech. rep., Feb. 01 1995.

[MVPC00] MARTÍNEZ-VERDÚ F., PUJOL J., CAPILLA P.: Calculation of the color-matching functions of digital cameras from their complete spectral responsitivities. In *Proc. CIC* (Nov. 2000), pp. 211–216.

[MVPC03] MARTINEZ-VERDU F., PUJOL J., CAPILLA P.: Characterization of a digital camera as an absolute tristimulus colorimeter. *J. IS&T 47*, 4 (2003), 279–374.

[NFG07] NORMAND C., FORNARO P., GSCHWIND R.: Automated digital camera sensor characterization. In *SPIE/IS&T EI* (2007), vol. 6502.

[PAJ01] POINTER M. R., ATTRIDGE G. G., JACOBSON R. E.: Practical camera characterization for color measurement. In *PICS* (2001), pp. 246–251.

[RBS99] ROBERTSON M. A., BORMAN S., STEVENSON R. L.: Dynamic range improvement through multiple exposures. In *Proc. IEEE ICIP* (1999), vol. 3, pp. 159–163.

[RSSF02] REINHARD E., STARK M., SHIRLEY P., FERWERDA J.: Photographic tone reproduction for digital images. *ACM Trans. Graph 21*, 3 (July 2002), 267–276.

[TAHL07] TALVALA E.-V., ADAMS A., HOROWITZ M., LEVOY M.: Veiling glare in high dynamic range imaging. *ACM Trans. Graph. 26*, 3 (2007), 37.

[Yam06] YAMADA T.: Ccd image sensors. In *Image Sensors and Signal Processing for Digital Still Cameras*, Nakamura J., (Ed.). CRC Press, Broken Sound Parkway, 2006, pp. 95–141.